Title
ENERGY-LEVEL SYSTEMATICS OF ODD-MASS LANTHANUM ISOTOPES; A NEW COUPLING SCHEME

Authors
Leigh, J.R.
Nakai, K.
Maier, K.H.
et al.

Publication Date
1972-12-01

Submitted to Nuclear Physics

LBL-1601
Preprint c.1

ENERGY-LEVEL SYSTEMATICS OF ODD-MASS LANTHANUM ISOTOPES; A NEW COUPLING SCHEME

J. R. Leigh, K. Nakai, K. H. Maier, F. Pühlhofer,
F. S. Stephens, and R. M. Diamond

December 1972

Prepared for the U. S. Atomic Energy Commission
under Contract W-7405-ENG-48

ENERGY-LEVEL SYSTEMATICS OF ODD-MASS LANTHANUM ISOTOPES; A NEW COUPLING SCHEME†

J. R. Leigh††, K. Nakai‡, K. H. Maier‡‡, F. Pühlhofer‡‡‡, F. S. Stephens, and R. M. Diamond

Lawrence Berkeley Laboratory
University of California
Berkeley, California 94720

December 1972

Abstract

Heavy-ion reactions have been used to populate states in the odd-A La nuclei (A = 125 → 137). The γ-ray spectra indicate strong population of a band based on the $11/2^-$ state of each isotope. The character of this band indicates a new type of coupling, and can only be explained if the state has a prolate deformation. This is in contrast to earlier suggestions of oblate shapes for these nuclei.

†Work performed under the auspices of the U. S. Atomic Energy Commission.

††Present address: Department of Nuclear Physics, Australian National University, Canberra, Australia.

‡Present address: Department of Physics, University of Tokyo, Tokyo, Japan.

‡‡Present address: Hahn-Meitner Institute, Berlin, Germany.

‡‡‡Present address: Department of Physics, University of Marburg, Marburg, Germany.

NUCLEAR REACTIONS $^{130,128,126,124,122}Te(^{11}B,4n\gamma)$ $^{137,135,133,131,129}La$, E = 40,45,50,52.5,56.5 MeV; $^{124}Sn(^{14}N,5n\gamma)^{133}La$, $^{120,118,116}Sn(^{14}N,3n\gamma)^{131,129,127}La$, E = 50.5,53,58,62,64.8,67,68.5,72,76 MeV; and $^{112}Sn(^{16}O,2np\gamma)^{125}La$, E = 72,76,82,88,94 MeV; measured $\sigma(E_\gamma,\theta)$, α_K. $^{125,127,129,131,135,137}La$ deduced levels, J, π. Enriched targets. Ge(Li) detector.

1. Introduction

The neutron-deficient nuclei with $Z > 54$, $N < 78$ have been extensively studied since this was first proposed as a new region of deformation[1]). The energy levels of the ground-state rotational bands[2,3,4]) and the life-times of the first 2^+ states[4,5,6]) of some of these doubly-even nuclei support the suggested deformation. Theoretical calculations[7,8,9]) of the shapes of nuclei in this region have indicated competition between oblate and prolate deformations, the oblate shape being slightly more stable in refs. [7,8]), though the reverse is true in ref. [9]) where hexadecupole deformation is included. The theoretical calculations suggest that these nuclei might be extremely soft to γ-vibrations. It is possible, therefore, that some of the observed E2 enhancement arises from dynamic effects rather than static deformations.

The possibility of determining the sign of the nuclear deformation from studies of very neutron-deficient doubly-even nuclei is remote. However, studies of odd-A nuclei offer two possible methods which are relatively simple experimentally. These are:

1) determining the sign of the mixing ratio δ(E2/M1) for the cascade transitions in rotational bands. The rotational model then predicts the sign of the quadrupole moment if information on the magnetic moment of the band is available. This possibility has been recently discussed[10]).

2) determining the spins and parities of the lower-lying quasi-particle states. This ordering depends critically on the sign of the nuclear deformation, and if states can be assigned to definite Nilsson orbitals the sign of the deformation may be determined.

The odd-A nuclei in this region have recently been studied by several authors, and the second of the above methods has been used to deduce the nuclear shape. The existence of low-lying $11/2^-$ levels, assigned as the [505] Nilsson state, in ^{129}La and ^{131}La has been used to support the proposed oblate deformation[11,12]). The occurrence of levels in ^{127}Cs with different signs of deformation has been postulated[13]). Isomers in the odd-N isotopes ^{125}Ba and ^{127}Ba have been observed[14]) and again interpreted as arising from oblate deformation. It should be stressed that the arguments supporting a negative deformation parameter have generally been based on the assignment of only one $11/2^-$ level in each nucleus. In contrast to these data, an isomer with an anomalously large prolate deformation has been reported in ^{133}La (ref. [15])).

It should be noted that such results are not as definitive as might be hoped. For example, in the present case a low-lying $11/2^-$ state might be the [505] Nilsson level, as has been suggested, and so indicate an oblate shape, or it might be the $11/2^-$ level of the band based on the [550] $\Omega = 1/2$ Nilsson state. The latter state has a large negative decoupling parameter, and so results in a distorted band with the 11/2 member lying low if on the prolate side. Thus, the mere occurrence of a low-lying $11/2^-$ level really does not decide between oblate and prolate shapes.

But the results of an in-beam study of the rotational band built on this level may allow a decision to be made. An oblate nucleus should show a normal rotational band with M1-E2 cascade and E2 cross-over transitions, while the $\Omega = 1/2$ band should show a simpler cascade made up only of E2 radiations. A schematic illustration of these possible level spacings and transitions is shown in fig. 1. With this in mind, a sequence of odd-mass La isotopes from A = 125 to 137 were studied by in-beam spectroscopic techniques following (HI,xn) reactions.

2. Experimental Method

The reactions used are indicated in Table 1; the Berkeley HILAC provided the heavy-ion beams. The beam pulses, normally 5 ms long with a repetition rate of 36 times/s can be further chopped using an electrostatic deflector system in order to provide beam bursts as short as 0.25 μs with continuously variable repeat intervals ($\geqslant$ 2.5 μs). This facility was used to study isomeric decays. Self-supporting and lead-backed targets of isotopically enriched materials were used, and were typically 1-2 mg/cm^2 in thickness.

Singles γ-ray spectra were recorded both in-beam and between beam pulses, using a Ge(Li) detector at 90° to the beam direction. Excitation functions were performed for all the isotopes studied and provided a unique assignment of the mass. In some cases angular distributions were performed using two Ge(Li) detectors, one of which was fixed and used as a monitor. The method has been described in ref. [16]).

It is possible by half-life considerations alone to restrict the 'prompt' transitions ($\tau_{1/2} < 20$ ns) observed to E1, M1 or E2 multipolarities. The method of population of the states[17]) generally implies that the observed γ-rays decay from a state of higher spin to one of lower spin. The following "stretched" cascades and their characteristic angular distributions are possible:

(i) stretched E2 ($I \rightarrow I-2$) transitions for which the angular distribution coefficients typically lie in the range $+0.2 \leqslant A_2 \leqslant +0.5$.

(ii) pure $\lambda = 1$ transitions ($I \rightarrow I-1$) for which A_2 has about the same magnitude as in (i) but is of opposite sign. The large hindrance factor associated with E1 transitions is usually sufficient to produce a measurable half-life and thus distinguish M1 from E1 transitions.

(iii) (I → I-1) mixed E2/M1 transitions; when δ is positive and small, an essentially isotropic distribution results, and when δ is negative, large nagative A_2's are expected ($A_2 < -0.5$).

Only in cases of very large E2/M1 admixtures can any ambiguity arise, and such δ's are not common for rotational transitions. Frequently, therefore, measurements at only two angles, usually 0° and 90°, are sufficient to determine the γ-ray multipolarity, and such studies were made in the cases of ^{127}La, ^{129}La, and ^{135}La.

Two Ge(Li) detectors, placed opposite each other and at 90° to the beam direction, were used for γ-γ coincidence measurements. A conventional fast-slow system was used incorporating a time-to-amplitude converter (TAC). The data were stored event-by-event on magnetic tape using a PDP-7 computer system. Each event is characterized by four parameters: the two γ-ray energies; the fast-timing signal from the TAC; and a slow-timing signal indicating when the coincidence occurred relative to the beam pulse. Storage of the TAC output enables measurement of half-lives in the range 30-500 ns, and also permits subtraction of random coincidence events. The slow-time parameter enables coincidence events associated with long-lived β-decay products or isomers to be recognized.

Out-of-beam conversion-electron spectra were recorded in the case of ^{131}La, using the chopped-beam facility to study the 170 μs isomer decay. A solenoidal spectrometer with a cooled Si(Li) detector was used for this purpose. Typical resolution for the 624 keV conversion line of ^{137}Cs was 3.5 keV.

In the case of ^{125}La, γ-ray spectra were recorded in coincidence with charged particles evaporated from a Ce compound system. Details of the method are discussed in ref.[18]).

3. Results

Typical γ-ray spectra are shown in figs. 2 and 3. The results are summarized in Table 2. For each isotope we have listed the γ-ray energies, the relative transition intensities, the angular distribution coefficients when determined, the γ-ray multipolarities and the transition assignments. The dominant feature of the spectra associated with the lighter isotopes studied is a sequence of strong γ-rays which closely resembles the γ-ray spectra of the ground-state band of the neighboring doubly-even Ba isotopes. In the cases where angular distribution measurements were performed, these transitions were found to be consistent with stretched E2 assignments. Even in the heaviest isotopes studied, ^{135}La and ^{137}La, there is one strong transition which is consistent with a stretched E2 assignment and whose energy is very close to the $2^+ \rightarrow 0^+$ γ-ray of the doubly-even Ba core, i.e., ^{134}Ba and ^{136}Ba, respectively. The γ-γ coincidence measurements showed that all these stretched E2 transitions were in coincidence with each other, and their relative transition intensities indicated their time ordering. The bands thus established are shown in fig. 7 where they are compared to the ground bands of the doubly-even Ba neighbors.

With ^{125}La and ^{127}La the only strong γ-rays observed were assigned to the stretched E2 cascade sequence. In ^{129}La this same band was a dominant feature and appeared to be based on an isomeric state with a half life of 0.56 s. The delayed transitions were the only other strong ones seen and were essentially equal in intensity to the lowest member of the band. In the comparison of these intensities, corrections were made for internal electron conversion and also for the timing relationship between the in-beam and out-of-beam spectra. The decay of this isomer has been studied previously[11,12]. The

54.5 keV transition reported in ref. 12) is generally seen in neutron evaporation reactions studied with Ge(Li) detectors and arises from ^{73m}Ge, which has a half life of 0.54 s. The decay scheme of the isomer is shown in fig. 4a.

The ^{131}La spectrum again shows the doubly-even-like band to be dominant, and again the only other strong transitions are associated with the decay of an isomeric state, $T_{1/2}$ = 170 μs. An isomeric decay has been reported previously[12]), though the γ-ray multipolarities were not established. Previous workers observed only two γ-rays, of energies 170 keV and 109 keV, with the 170 μs half life. Two other γ-rays were observed in our work and are possibly associated with the isomer. A 196 keV transition showed a half life of 190±30 μs, and a 26 keV γ-ray had a half life in the range 10-500 μs. Energy sums suggest that the 170 keV and 26 keV transitions form a cascade sequence, with the 196 keV γ-ray arising from the cross-over transition. The 196 keV transition is about 20 times weaker than the 170 keV line, while the intensity of the 26 keV transition depends strongly on its multipolarity. In a separate experiment we studied the decay of ^{131}Ce to ^{131}La. The level scheme deduced from that decay indicates states at 26 keV and 196 keV. The 170 keV/196 keV intensity ratio is the same in both the ^{131}Ce decay and the 170 μs isomer decay, suggesting that both γ-rays arise from the same state. The isomer decay scheme deduced is shown in fig. 4b.

Only the 109 keV and 170 keV transitions were observed in the conversion electron spectrum; the data are summarized in Table 3. The K/(L+M) ratios are determined directly from the electron spectrum; the experimental α_K is determined assuming the decay scheme of fig. 4b, i.e., assuming the 170 keV and 109 keV transitions have approximately the same total intensities.

The ^{133}La spectrum is rather complex. There are two strong transitions which are obvious candidates for the lower two members of the band which was observed in the lighter isotopes. These two transitions are in coincidence with each other and precede a 60 ns delay. The delay is associated with a level at 535 keV whose decay is shown in fig. 4c. A very large proportion of the cross-section leads to population of this state, which is also observed in the decay of ^{133}Ce (ref. 19-21). Other strong γ-rays are observed which are not fitted into the level scheme. There is considerable conflict between the spin assignments made in this work and those of ref. [20]). Assignments made by several workers are indicated in fig. 4c and are discussed later.

The ^{135}La spectrum shows several strong γ-rays which arise from an isomeric state, $T_{1/2} \simeq 50$ ns, at 2.7 MeV. About 40% of the cross-section leads to population of this state. The state decays via seven cascade γ-rays to ground. No other delays $\gtrsim$ 20 ns are observed in the cascade sequence. The relative intensities of the transitions determine their ordering, indicating the 470 keV transition to be the isomeric one. The isomeric transition has also been identified by studying the time-spectrum of each γ-ray in coincidence with all γ-rays above about 800 keV. Since no γ-rays above this energy are observed in the isomeric decay, the time spectrum obtained is that due only to transitions preceding each γ-ray studied. The time spectrum not showing a prompt component is then associated with the isomeric transition, and the 470 keV transition was thus identified. Angular distribution measurements were performed and the results are shown in Table 2. The isomeric decay scheme is shown in fig. 5.

The spectrum associated with ^{137}La shows strong γ-rays from the decay of the well-established $11/2^-$ state at 1.004 MeV. Only one other strong transition at 782 keV has been assigned. This is in coincidence with the γ-rays from the $11/2^-$ state and has an anisotropy consistent with a stretched E2 transition.

4. Discussion

4.1. SPIN AND PARITY ASSIGNMENTS

Since all types of measurements have not been performed for all isotopes, it is necessary to rely on energy-level systematics in making some of the assignments. In order to establish the systematic trends, those assignments in which we have the most confidence are presented first. The systematics obtained seem very convincing, though the assignments for the levels in ^{135}La above 1.5 MeV must be considered tentative.

4.1.1. The ^{131}La nucleus. The ground-state spin has been measured[22]) as 3/2 and is most likely to have positive parity. The isomeric state decays by three cascade γ-rays to ground (fig. 4b). The 109 keV and 170 keV transitions are clearly established as M2 and M1 respectively, by our electron data (Table 3). The 26 keV transition has the same total intensity as the 170 keV only if it has M1 multipolarity. The 196 keV multipolarity has not been measured, but since it competes unfavorably with the 170 keV transition it is most likely to have E2 character. Thus, the spin sequence shown in fig. 4b is suggested. If we estimate the M1-E2 mixing ratio of the 170 keV transition assuming it has an E2 component with the same strength as the 196 keV transition, we obtain δ^2(E2/M1) = .02. This value is in reasonable agreement with the $7/2^+ \rightarrow 5/2^+$ transition in ^{133}La or ^{135}La and supports the spin assignments. The stretched E2 sequence based on the $11/2^-$ state gives rise to a band with spins $15/2^-$, $19/2^-$, $23/2^-$, etc.

Recently, studies of the (α,t) transfer reaction on some doubly-even barium isotopes have been carried out[23]). States assigned as $5/2^+$, $7/2^+$, and $11/2^-$ are the only levels strongly populated in the odd-A La isotopes between masses 131 and 137. These results confirm the $11/2^-$ assignnment for this isomer.

4.1.2. The ^{129}La nucleus. The ground-state spin of this nucleus is expected to be the same as that of the neighboring ^{131}La, i.e., $3/2^+$. The 0.56 s isomer has been shown to decay by an E3-M1 cascade sequence[11]). This establishes the spin and parity of the isomeric state as $11/2^-$. The prominent E2 sequence decaying to the isomer leads to the $15/2^-$, $19/2^-$, etc. assignments for the higher states.

4.1.3. The ^{137}La nucleus. The well-known $11/2^-$ state was strongly populated, and only one strong transition of 782 keV was observed to feed this level. This γ-ray has the characteristics of a stretched E2 transition and has been assigned as $15/2^- \rightarrow 11/2^-$. Again, the (α,t) reaction[23]) strongly populates just the well-known $5/2^+$, $7/2^+$, and $11/2^-$ states.

4.1.4. The ^{127}La and ^{125}La nuclei. In both these cases only the stretched E2 band is observed. Comparison with the doubly-even Ba neighbors and the heavier La isotopes discussed above, strongly suggest we are seeing the γ-rays from the same sequence of states with spins $11/2^-$, $15/2^-$, $19/2^-$, etc. A study of the ^{127}La decay was undertaken, and states in ^{127}Ba were populated which displayed features typical of a rotational band. The most likely spin assignments for the ^{127}Ba states are not inconsistent with an $11/2^-$ assignment for the ^{127}La parent.

The energy level systematics indicate that with a decrease in A, the $11/2^-$ state drops whilst the $5/2^+$ and $7/2^+$ states rise, so it is not surprising that the $11/2^-$ has dropped below both these states in ^{127}La. The decay modes open to the $11/2^-$ state are then β-decay or M4 γ-decay to the $3/2^+$ state if the latter remains below the $11/2^-$ state. The single-particle half life for an M4 transition is $\approx 10^7$ s, therefore, the observed β-decay with $T_{1/2}$ = 5.0±0.5 m would be strongly favored. In ^{125}La the $11/2^-$ state may even have become the ground state.

4.1.5. The ^{133}La nucleus. The ^{133}Ce decay has been previously studied and the level scheme shown in fig. 4c deduced[19-21]). The isomeric state at 535 keV is also strongly populated in our in-beam work. The (HI,xn) reaction introduces very high angular momentum into the compound system; the subsequent decay by emission of neutrons and γ-rays has been discussed[17]), and the decay mechanism generally implies that at a given (low) energy, the state with highest spin is most heavily populated. The strong population of the 535 keV state clearly suggests, then, that this state has higher angular momentum than the levels below it. It would, therefore, be very surprising if its spin were as low as 3/2 as suggested in refs. [19-21]).

Two of the stronger γ-rays in the spectrum are shown by delayed γ-γ coincidences to precede the 60 ns delay associated with the 535 keV level. The energies of these γ-rays are just those expected from the systematics for the lower members of the stretched E2 band. A third transition, not observed in delayed coincidence, has been assigned to the band on energy and intensity considerations. The agreement with the systematic trends and the degree of population of the 535 keV level leads to the assignment of $11/2^-$ for this state. The lower states would then have the spins shown in fig. 4c. No angular distribution data or conversion-electron data were taken in this work. However, conversion coefficients have previously been determined from the ^{133}Ce decay[20]). Our re-assignments of the spins below the 535 keV level are entirely consistent with the electron data. Table 4 compares the experimental and theoretical conversion coefficients for the assignments of this work and of ref. [20]). Our M2 assignment for the 404 keV γ-ray looks more reasonable than the E1(+M2) of ref. [20]), and the M1 and E2 predictions for the 477 keV γ-ray cannot be distinguished. If the 404 keV transition were E1, there would be a large hindrance factor of 4×10^8 associated with it. An attempt was made to explain this[15]) by assuming a shape-hindered transition. However, the 58.4 keV E1 branch from the same level has a hindrance of only 1.3×10^5, which is typical for E1 transitions, but should also be shape hindered if one uses the arguments of ref. [15]). Our assignments remove this difficulty, making the 404 keV γ-ray an M2. The hindrance factor associated with it is then ~ 50 in very good agreement with the $11/2^- \rightarrow 7/2^+$ transition in ^{131}La which is hindered by ~ 100.

Further support for our assignments appears in ref. [24]), where the spin of the 130.7 keV level has been suggested to be $7/2^+$ and the 97 keV state to be $3/2^+$. These assignments are based on systematics of the M1 hindrance and E2 enhancement factors for the $7/2^+ \rightarrow 5/2^+$ transition in a series of La isotopes. The systematic results of the (α,t) reaction[23]) most strongly suggest an assignment of $11/2^-$ to a level at about 535 keV whilst our in-beam γ-ray work shows this to be the same level that is observed in the β-decay studies. The spin and parity assignments of this work and refs. [20,23,24]) are compared in fig. 4c.

The ^{133}Ce β-decay data [20]) could be explained if the observed 5.4 h activity is associated with a high-spin state of ^{133}Ce rather than the $1/2^+$ state proposed in ref. [20]). High-spin states are known in ^{139}Ce and several odd-A Ba isotopes. The tendency is for these states to drop in energy with decreasing mass. It is, therefore, plausible that the $11/2^-$ state in ^{133}Ce is sufficiently low in engergy to have become a β-decaying isomer. Some re-evaluation of the decay data might be in order in the light of the present data and that of refs. [23,24]). The large hindrance associated with the $9/2^+ \rightarrow 7/2^+$ transition will be discussed later.

The nuclear moments of the 535 keV level have been reported[15]). There has been some difficulty in the interpretation of the observed magnetic moment. However, since we believe the spin of the state is $11/2^-$, a re-evaluation of this moment is in order. The observed quantity in ref. [15]) must be the g-factor of the state, which would be $g = \mu/I = 1.4$. This is very close to the Schmidt value for the $h_{11/2}$ proton ($g_{Schmidt} = 1.42$). The interpretation of the $11/2^-$ state as discussed below indicates mainly $h_{11/2}$ single-particle character. The single-particle moment for the $h_{11/2}$ proton in this region is calculated to be $g_{cal} = 1.44$, with $\delta g_s = -0.07$. The latter value was calculated with the theory of Arima and Horie[25]).

While the difficulty in the magnetic moment is resolved, the experimental result on the quadrupole moment is still difficult to explain. The deformation parameter deduced from it was anomalously large, $\beta = 0.47$. The re-evaluation with the new spin assignment yields an even larger value of Q and β. This is unreasonable, and the measured quadrupole frequency needs to be checked.

4.1.6. <u>The ^{135}La nucleus</u>. The ^{135}Ce decay has been well studied. Only one γ-ray common to both this decay and to the in-beam work has been observed. This is the 119 keV $7/2^+ \rightarrow 5/2^+$ transition, the ground-state being well established as $5/2^+$. The angular distribution coefficients, listed in table 2, are the only available data on which spin assignments can be made. The known 119 keV transition has an essentially isotropic distribution. This is expected from its established E2/M1 character with $|\delta| = .2$ (Ref. [26])) if the sign of δ is positive. Most of the other strong γ-rays are associated with the decay of the isomer at 2.7 MeV, and only these will be discussed. Four of the transitions have positive A_2's with small negative A_4 coefficients. These are generally consistent with stretched $\lambda = 2$ transitions. The other three transitions have negative A_2's and are most likely to contain mixtures of $\lambda = 2$ and $\lambda = 1$. Thus, the spin sequence shown in fig. 5 is reasonably well established though parity assignments are based on plausibility arguments and systematic trends, and must therefore be considered tentative.

The M2 possibility for the positive A_2 transitions seems unlikely, the half lives of the states ruling out any such transition with an enhancement factor less than about 3. It is most probable, therefore, that these are stretched E2 transitions. Their A_2's can be used to calculate the degree of nuclear alignment by comparison with the tables of Yamazaki[26]) which give the angular distribution coefficients for complete alignment. The alignment thus derived is attenuated by a factor between 2 and 3, the attenuation factor increasing with the excitation energy of the state. This apparently surprising behaviour may be due to the fact that the higher states are populated predominantly by decays from the isomeric state, and decays through this state may be seriously attenuated due to its relatively long half-life. We have used attenuation factors of 2.3±0.2 for the 202 keV line and 2.8±0.4 for the 133 keV and 470 keV transitions to correct the observed values of A_2. Both the 133 keV and 202 keV γ-rays than have corrected values of A_2 typical of mixed $\lambda = 1$ and $\lambda = 2$ transitions with $\delta\left(\frac{\lambda = 2}{\lambda = 1}\right)$ equal to 0.1±0.1. The states from which these γ-rays arise have half-lives < 20 ns. A 1% M2 admixture in the 133 keV transition would imply an enhancement factor for the M2 component of > 3. This is unlikely and so we assign the 133 keV transition as E2/M1. The 202 keV could be E2/M1 or M2/E1, either assignment implying a spin 11/2 for the 786 keV state. The (α,t) data[23]) show the $11/2^-$ state to lie very close to this energy and the 786 keV state is thus assigned as $11/2^-$.

The very large negative A_2 coefficient of the 470 keV transiton can only be obtained from a $\lambda = 1$ and $\lambda = 2$ mixture with $\delta \approx 1.0$, higher multipolarities being excluded by the half-life. The half-life is consistent with an M2/E1 mixture with hindrance factors of ~1 and $\sim 4 \times 10^7$ for the M2 and E1 components, respectively.

If we assume the 786 keV state is indeed the $11/2^-$ state, then the preceding 593 keV E2 transition is a good candidate for the $15/2^- \rightarrow 11/2^-$ member of the band observed in the lighter isotopes. Based on the doubly-even nuclei, the $19/2^-$ member of this band would be expected about 400 keV higher than the observed 19/2 state. Its direct population would then be relatively weak and transitions from it would not be seen in-beam. Since the $19/2^-$ band member is also anticipated to lie close to the observed 23/2 state at 2.13 MeV, it would not be populated in the isomer decay.

The observed $19/2^-$ state at 1.75 MeV possibly has a similar structure to the $19/2^-$ isomeric state in ^{135}Cs (Ref. [28])) at 1.63 MeV excitation energy. At least the ^{135}Cs state gives a clear indication of the energy at which high-spin 3-quasi-particle states are expected in this region of A.

Several strong transitions are observed which feed the isomeric state, but no attempt has been made to assign multipolarities to these transitions.

4.1.7. The ^{139}La nucleus. No attempt was made to study levels of this nucleus in our work, but well-established levels with spin and parity $7/2^+$, $5/2^+$, and $11/2^-$ aid in establishing the systematics. Again these are just the states strongly populated in the (α,t) reaction of ref. [23]).

4.2. THE POSITIVE-PARITY STATES

The energy-level variation of these states is shown in fig. 6. States with spins 3/2, 5/2, 7/2, and 9/2 have been identified in ^{131}La to ^{137}La. The $9/2^+$ state is not known in ^{139}La and only the $3/2^+$ and $5/2^+$ levels have been observed in ^{129}La. The (α,t) proton transfer reactions[23]) consistently populate only the $5/2^+$, $7/2^+$, and $11/2^-$ states. Levels populated by these reactions should be predominantly particle-states. This effectively rules out the possibility of a static oblate shape since the $7/2^+$ state would certainly lie below the Fermi surface for such a deformation. Thus, the $5/2^+$ and $7/2^+$ states must be associated with either a static prolate deformation or a spherical (soft-vibrating) nucleus. The $3/2^+$ and $9/2^+$ states were not observed, or observed only weakly, in the transfer work and may be either hole-states or collective states.

If we assume the behavior of the positive parity states in fig. 6 to be interpretable from a strong-coupling scheme, the 3/2, 5/2, and 7/2 states can be assigned to specific Nilsson orbits. The general trends of such a description are in qualitative agreement with fig. 6, assuming increasing deformation with decreasing A. However, there are several inconsistencies. One is that there are several particle-states below 1 MeV which should then be observed in the single-proton transfer reactions, but are not seen. More serious, such a scheme leads to assignment of the $5/2^+$ and $7/2^+$ levels to Nilsson states arising from the $g_{7/2}$ shell, i.e., $5/2^+[413]$ and $7/2^+[404]$. But then the large M1 hindrance associated with transitions between these levels[24]) is difficult to explain (see Table 5). Finally, the presence of the $9/2^+$ level is not expected from such a strong-coupling model.

The M1 hindrance associated with the $7/2^+ \rightarrow 5/2^+$ transition in the odd-A La nuclei has previously been ascribed[24]) to the 'ℓ- forbiddenness' of M1 transitions between the $g_{7/2}$ and $d_{5/2}$ levels. If this is the source of hindrance, then the soft-vibrating picture of the nucleus seems appropriate at least down to ^{131}La. The levels of such a nucleus have been described[29]) using pairing-plus-quadrupole interactions. The calculated results for a series of light Cs isotopes show striking similarities to the states in fig. 6. Indeed, except that the $3/2^+$ state appears too high in the calculations, the agreement is remarkable. With this description the $5/2^+$ and $7/2^+$ states have largely single-particle character, whilst the other states involve core-excitation. In particular, the $9/2^+$ level would then be a $5/2^+$ particle coupled to a 2^+ core-excitation. This is supported by the values of the ratios, $R_{exp}/R_{s.p.}$ with R = T(E2; 9/2 → 5/2)/T(M1; 9/2 → 7/2), given in Table 5, and also by the energies of the $9/2^+ \rightarrow 5/2^+$ transitions listed there which are within 20 keV of the corresponding $2^+ \rightarrow 0^+$ transition of the doubly-even core nuclei. The properties of the positive-parity states seem, then, to be well described by this model. A new scheme will be presented below for the negative-parity states and will be shown to describe them very well; it remains to be seen what such a model will yield for these positive-parity levels.

4.3. THE NEGATIVE-PARITY BAND

Transitions associated with this band are reasonably well established in the lighter isotopes, though only one transition has been assigned in the two heavier nuclei, ^{135}La and ^{137}La. The bands are shown in fig. 7 where they are compared with the doubly-even Ba isotopes. Clearly, these bands do not display the characteristics typical of an odd-A rotational band based either on a Ω = 11/2 state (oblate) or a (distorted) Ω = 1/2 band (prolate), as originally expected, and illustrated in fig. 1. That is, for the former case, a series of M1-E2 cascade and E2 cross-over transitions should be seen, with the 15/2 → 11/2 spacing more than 4 times the 2 → 0 spacing in the ground band of the doubly-even Ba core nucleus. For the latter case, only a stretched E2 cascade should be seen, but the 15/2 → 11/2 spacing should be about twice the energy of the 2^+ level in the doubly-even core. However, neither of these cases are found. What is observed in fig. 7 is a stretched E2 cascade having transition energies which very closely resemble those of the Ba core nucleus itself.

A possible explanation for this result is that we are observing weak coupling of an $h_{11/2}$ proton to the core[30]). This would provide a multiplet of nearly degenerate levels at each of the states of the core nucleus, and the sequence of the highest-spin members of each multiplet would yield a stretched E2 cascade like that observed. However, we do not believe this is the answer for a number of reasons. Since the multiplet members should not be exactly degenerate, more than one transition should be observed between the core states, even though the highest-spin members are favored in the (HI,xn) reaction. But only one transition is seen in every case and in each nucleus. In addition, the level spacings in the Ba core are small enough to indicate that the multiplet splittings would not be small compared to the core spacings.

We believe that a new coupling scheme, which we call "rotation-aligned", is the explanation for the band observed. A preliminary account of this has already been published[31]), but we would like to give here the physical background for the scheme, and to amplify the description. Consider a particle coupled to an axially-symmetric rotation core. The Hamiltonian can be written

$$H = H_{intr} + H_{rot} = H_{intr} + \frac{\hbar^2}{2\mathcal{J}} \vec{R}^2 \qquad (1)$$

By means of the relation, $\vec{R} = \vec{I} - \vec{j}$, eq. (1) may be expressed in a form appropriate to the use of wave functions of the strong-coupling limit where Ω is a good quantum number,

$$H = H_{intr} + \frac{\hbar^2}{2\mathfrak{I}} [I(I + 1) + \langle j^2 \rangle - 2\Omega^2] + H_c \quad (2)$$

with

$$H_c = - \frac{\hbar^2}{2\mathfrak{I}} (I_+ j_- + I_- j_+) \quad (3)$$

H_{intr} must also be specified, as for example, by the Nilsson model. We shall use, as before[31]), a linear approximation to the Nilsson expression,

$$E(\Omega) = E_o(n\ell j) + \frac{206\beta}{A^{1/3}} \left[\frac{3\Omega^2 - j(j + 1)}{4j(j + 1)} \right] \quad (4)$$

where the constant, 206, has been determined to give the best fitting to the $h_{11/2}$ protons in the complete Nilsson diagram.

In the limit of strong coupling, the term H_c becomes vanishingly small; Ω becomes a good quantum number, and each state involves a distribution in R. Thus, eq. (2) approaches the expression, $\frac{\hbar^2}{2\mathfrak{I}} I(I + 1)$ + constant, namely, that of the Bohr-Mottelson rigid rotor[32,33]). This reflects the fact that the most efficient way to carry angular momentum in a strongly-deformed nucleus is by rotation of the core; $\hbar^2/2\mathfrak{I}$ is small, and the different projections of the particle angular momentum have relatively large energy separations.

But as the deformation, β, is made smaller, the value of $\hbar^2/2\mathfrak{I}$ goes up, so that there comes a point where it is cheaper energetically to vary the projection of the particle angular momentum than the rotational angular momentum of the core. Near this limit, the so-called Coriolis term, H_c, becomes very large and H_{intr} becomes small. This corresponds to the weak-coupling limit[30]), where (nearly) degenerate multiplets of levels occur at the spacings of the core excitations. Now R is a good quantum number, but each state has a distribution of Ω values.

However, neither of these limits corresponds very well to the actual situation with the odd-mass La nuclei. Calculations made by exactly diagonalizing eq. (2) indicate that for an odd $h_{11/2}$ proton in La the strong-coupling limit is approached only for $\beta > 0.4$ and the weak-coupling limit for $\beta < 0.08$, while the real nuclei have intermediate deformations of 0.15-0.25. In the real intermediate case, it might be expected that the total angular momentum of the nucleus would be carried most efficiently by a more equal sharing between the particle and core motions. This is best done if their rotational axes are nearly aligned (such states go over eventually into the highest-spin member in each weak-coupling multiplet). Hence, the origin of the name, "rotation aligned", for this coupling scheme. The force which drives a nucleus from strong coupling into the new scheme is the Coriolis force, and when the particle and core angular momenta are nearly aligned, the Coriolis force becomes very small and there is no longer any appreciable coupling between the particle and the rotation of the core. Thus, the differences in energy for these levels are just those of the core itself. The result is observation of a gamma-ray cascade, $\rightarrow j+4 \rightarrow j+2 \rightarrow j$, consisting of stretched E2 transitions very similar to those of the ground bands of the neighboring doubly-even core nuclei. This band of levels has been called the "decoupled" band.

For this band, spatial alignment of the particle angular mementum with that of the deformed core requires, in terms of the strong-coupling wave functions, contributions from all possible Ω-components for a given j. But the most important one will be that of $\Omega = 1/2$ and the least important will be $\Omega = j$; this can be easily understood since the rotation axis is at right angles to the nuclear symmetry axis. Thus, for this new scheme to be possible, the Fermi surface must not be very far from the $\Omega = 1/2$ level. This means low with respect to the $h_{11/2}$ shell on the prolate side, and high on the oblate side. An additional requirement is that β cannot be too large, as then the level scheme will go over into the strong-coupling model. These requirements enable predictions as to where this scheme should occur, and help explain why there is a difference in behavior between the oblate and prolate sides as shown in fig. 8. When the Fermi surface approaches the $h_{11/2}$ shell from below, the $\Omega = 11/2$ state is lowest for large negative values of β, because that particle orbital best fits into the oblate potential. This yields a normal $\Omega = 11/2$ rotational band as shown on the far left in fig. 8. But as $|\beta|$ decreases through the region near 0.1 the nucleus switches rather rapidly from the strong-coupling to the weak-coupling scheme, skipping the new one because the lowest-energy orbital of the rotation-aligned scheme does not fit into the potential of the rotating oblate spheroid as well as those of other projections. Weak coupling yields the series of nearly degenerate multiplets shown around $\beta = 0$. But as the nucleus passes through $\beta = 0$ and becomes prolate, the new coupling scheme takes over from weak coupling for the reasons already described and because the high-spin member of each multiplet does fit well into the rotating prolate potential. Only at large values, $\beta > 0.3$, does this scheme slowly change into the strong-coupling model. If the Fermi surface moves up into the middle of the $h_{11/2}$ shell, the new coupling scheme has a hard time establishing itself because it requires a large proportion of the $\Omega = 1/2$ component. When the Fermi surface gets to the top of the $h_{11/2}$ shell, the behavior on the two sides reverses, and Coriolis decoupling appears on the oblate side, where $\Omega = 1/2$ dominates, again at intermediate values of β.

The previous discussion can also be turned around so that if one knows where the Fermi surface is and determines the nature of the band, i.e., whether deformation-aligned or rotation-aligned, the shape of the nucleus is determined. In the present examples of the odd-mass La nuclei (Z = 57), the Fermi surface is below the $h_{11/2}$ proton shell. As shown in fig. 7 , the bands built on the $11/2^-$ states are all decoupled. From fig. 8 , it can be seen that this requires that these nuclei be prolate with deformations in the range $0.1 \leqslant \beta \leqslant 0.3$. This is in contradiction to the conclusions of earlier workers, but we believe the evidence is very compelling.

In addition, we should point out that the type of behavior described above for the odd-mass La nuclei is certainly not restricted just to them. Any high-j shell should show this behavior under the proper conditions, and, in particular, the unique-parity levels in each shell should be candidates, as they have the highest value of j in that shell. Whenever the Fermi surface approaches such a shell from below on the prolate side or from above on the oblate side, the occurrence of a band j, j+2, j+4, ..., with spacing similar to those of the ground band of the neighboring doubly-even core nuclei might be expected. For example, under these conditions such behavior could occur for other $h_{11/2}$ odd-proton nuclei, for $g_{9/2}$ odd-proton and odd-neutron nuclei, and for $h_{11/2}$ and $i_{13/2}$ odd-neutron nuclei. Later papers will discuss a number of such examples that have been studied.

H has been emphasized that the new coupling scheme is not weak coupling, and we have derived it starting from the strong-coupling limit by including exactly the effects of the Coriolis interaction. This same intermediate-coupling scheme can be obtained by starting from the weak-coupling limit and including the effects of the particle-quadrupole deformation term, $\beta_2 Y_2$. Vogel[34]) described such a treatment, but considered only the diagonal terms. Recently the exact diagonalization starting from this limit has been performed[35]), yielding the same results given here and in the previous paper[31]).

Finally we should point out that although we believe this new coupling scheme is a good approximation to the actual behavior of a number of nuclei, such as the odd-mass La's, the calculations are obtained from diagonalization of eq. (2) which represents a rather simple model, namely, a single particle coupled to an axially-symmetric rotor of quadrupolar deformation. To whatever extent real nuclei are asymmetric (gamma deformation), show octupole, hexadecupole, and higher distortions, and are non-rigid, this simple picture will have to be modified. But the remarkable agreement of calculated behavior with experimental results for the La and other nuclei studied leads us to believe that the picture may not be very sensitive to these other effects.

5. Conclusion

We may summarize the experimental findings of this work as follows:

1) in each of the nuclei, $^{125-137}La$, a low-lying $11/2^-$ level has been observed (with help from the (α,t) studies of ref. [23]);

2) the in-beam spectroscopic work shows that above this $11/2^-$ state there are one or more states connected by strong, stretched E2 transitions, yielding on ascending sequence at levels $11/2^-$, $15/2^-$, $19/2^-$, ...;

3) the spacings of this band in each odd-mass nucleus are closely similar to those of the ground band of the neighboring doubly-even Ba core;

4) the $11/2^-$ state drops monotonically in energy from ~1.42 MeV in ^{139}La to perhaps becoming the ground-state in ^{125}La.

Features 2) and 3) above show that the properties of these $11/2^-$ bands are not those expected from either a strong- or weak-coupling scheme. But, all of the results can be encompassed by a new coupling scheme for a high-j particle bound to an axially-symmetric rotor. At moderate deformation the Coriolis interaction tends to decouple the particle from the symmetry axis of the nucleus and to align the particle angular momentum with that of the core. The lowest-lying high-spin levels will then form a sequence j, j+2, j+4,.... with energy spacings the same as those of the doubly-even core, just as is observed for the odd-mass La nuclei. To produce such a band, the Fermi surface must be near the $\Omega = 1/2$ Nilsson orbital. For the La isotopes, Z = 57, this can only be true if the nuclei are prolate. So, in disagreement with earlier workers, we conclude that the odd-mass La nuclei are prolate, not oblate.

References

1) R. K. Sheline, T. Sikkeland, and R. N. Chanda, Phys. Rev. Letters 7 (1961) 446

2) J. E. Clarkson, R. M. Diamond, F. S. Stephens, and I. Perlman, Nucl. Phys. A93 (1967) 272

3) D. Ward, R. M. Diamond, and F. S. Stephens, Nucl. Phys. A117 (1968) 309

4) A. Abdul-Malek and R. A. Naumann, Nucl. Phys. A108 (1968) 401

5) P. J. Pan, J. S. Horowitz, R. B. Moore, and R. Barton, Can. J. Phys. 44 (1966) 1029

6) W. Kutschera, W. Dehnhardt, O. C. Kistner, P. Kump, B. Pohv, and H. J. Sann, Phys. Rev. 5C (1972) 1658

7) K. Kumar and M. Baranger, Phys. Rev. Letters 12 (1964) 73

8) J. A. Arseniev, A. Sobiczewski, and V. G. Soloviev, Nucl. Phys. A126 (1969) 15

9) I. Ragnarsson and S. G. Nilsson, Colloquium on Intermediate Nuclei, Institut de Physique Nucléaire d'Orsay, Report IN 2 P3, 112 (1971)

10) K. Nakai, Phys. Letters 34B (1971) 269

11) K. F. Alexander, W. Neubert, H. Rotter, S. Chojnacki, Ch. Droste, and T. Morek, Nucl. Phys. A133 (1969) 77

12) T. W. Conlon and A. J. Elwyn, Nucl. Phys. A142 (1970) 359

13) T. W. Conlon, Nucl. Phys. A161 (1971) 289

14) J. M. D'Auria, H. Bakhru, and I. L. Preiss, Phys. Rev. 172 (1968) 1176

15) C. Gerschel, N. Perrin, and L. Valentin, Phys. Letters 33B (1970) 299

16) J. O. Newton, F. S. Stephens, R. M. Diamond, K. Kotajima, and E. Matthias, Nucl. Phys. A95 (1967) 357

17) J. O. Newton, F. S. Stephens, R. M. Diamond, W. H. Kelly, and D. Ward, Nucl. Phys. A141 (1970) 631

18) F. S. Stephens, J. R. Leigh, and R. M. Diamond, Nucl. Phys. A170 (1971) 321

19) H. Abou-Leila, C. Gerschel, and N. Perrin, Compt. Rend. 265 (1967) 1131

20) C. Gerschel, Nucl. Phys. A108 (1968) 337

21) C. Gerschel, J. P. Husson, N. Perrin, and L. Valentin, Int. Conf. on Properties of Nucl. States, Montreal (1969)

22) C. Ekström, private communication

23) K. Nakai, P. Kleinheinz, J. R. Leigh, K. H. Maier, F. S. Stephens, R. M. Diamond, and G. Løvhøiden, Phys. Letters; P. Kleinheinz, K. Nakai, and G. Løvhøiden, to be published.

24) R. Babadzhanov, V. A. Morozov, T. M. Muminov, V. I. Razov, and A. B. Khalkulov, Dubna Report JINR P6-5200 (1970)

25) A. Arima and H. Horie, Prog. Theor. Phys. 11 (1954) 509

26) Y. Nagai, M. Akiba, and K. Hisatake, J. Phys. Soc. Japan 29 (1970) 790

27) T. Yamazaki, Nucl. Data A3 (1967)

28) I. B. Häller and B. Jung, Nucl. Phys. 52 (1964) 524

29) L. S. Kisslinger and R. A. Sorensen, Rev. Mod. Phys. 35 (1963) 853

30) A. de Shalit, Phys. Rev. 122 (1961) 1530

31) F. S. Stephens, R. M. Diamond, J. R. Leigh, T. Kammuri, and K. Nakai, Phys. Rev. Letters 29 (1972) 438

32) A. Bohr, Dan. Mat. Fys. Medd. 26 (1952) no. 14

33) A. Bohr and B. R. Mottelson, Mat. Fys. Medd. Dan. Vid. Selsk. 27 (1953) no. 16

34) P. Vogel, Phys. Letters 33B (1970) 400

35) P. Kleinheinz, G. Løvhøiden, K. Nakai, and S. Harris, B.A.P.S. 17 (1972) 898

Table 1

Target	Reaction	Product	Energies used*
^{130}Te	(^{11}B,4n)	^{137}La	40,$\underline{45}$,50,52.5
^{128}Te	(^{11}B,4n)	^{135}La	40,45,$\underline{50}$,52.5,56.5
^{126}Te	(^{11}B,4n)	^{133}La	42,47,50,$\underline{52.5}$,56.5
^{124}Sn	(^{14}N,5n)	^{133}La	64.8,$\underline{68.5}$,72
^{124}Te	(^{11}B,4n)	^{131}La	50,$\underline{56.5}$
^{120}Sn	(^{14}N,3n)	^{131}La	50.5,$\underline{53}$,58
^{122}Te	(^{11}B,4n)	^{129}La	50,$\underline{56.5}$
^{118}Sn	(^{14}N,3n)	^{129}La	53,$\underline{58}$,$\underline{62}$,67,76
^{116}Sn	(^{14}N,3n)	^{127}La	52.5,$\underline{58}$
^{112}Sn	(^{16}O,2np)	^{125}La	$\underline{72}$,76,82,88,94

*Best energy is underlined.

Table 2

La Isotope	E_γ	Relative Transition Intensity	$A_2 = G_2A_2(max)$	Multi-polarity	Transition Assignment
125	240.9	100		(E2)[a]	$15/2^- \rightarrow 11/2^-$
	437.1	92		(E2)[a]	$19/2^- \rightarrow 15/2^-$
	604.3	97		(E2)[a]	$23/2^- \rightarrow 19/2^-$
127	252.1	100	.23±.03	E2 [b]	$15/2^- \rightarrow 11/2^-$
	458.6	72	.25±.04	E2 [b]	$19/2^- \rightarrow 15/2^-$
	630.9	40	.21±.06	E2 [b]	$23/2^- \rightarrow 19/2^-$
	779.9	15	.27±.16	E2 [b]	$27/2^- \rightarrow 23/2^-$
129	68.9	96		M1 [c]	$5/2^+ \rightarrow 3/2^+$
	104.8	106		E3 [c]	$11/2^- \rightarrow 5/2^+$
	170.5			M1 [c,d]	$(7/2^+ \rightarrow 5/2^+)$
	269.3	100	.24±.03	E2 [b]	$15/2^- \rightarrow 11/2^-$
	474.7	74	.29±.04	E2 [b]	$19/2^- \rightarrow 15/2^-$
	641.4	48	.22±.06	E2 [b]	$23/2^- \rightarrow 19/2^-$
	785	14	.21±.12	E2 [b]	$27/2^- \rightarrow 23/2^-$
131	26.	84		(M1)	$5/2^+ \rightarrow 3/2^+$
	108.9	108		M2 [e]	$11/2^- \rightarrow 7/2^+$
	169.6	100		M1 [c,e]	$7/2^+ \rightarrow 5/2^+$
	195.6	5		(E2)	$7/2^+ \rightarrow 3/2^+$
	244.8			(M1) [d]	$(9/2^+ \rightarrow 7/2^+)$
	335.6	100		(E2) [a]	$15/2^- \rightarrow 11/2^-$
	414.2			(E2) [d]	$(9/2^+ \rightarrow 5/2^+)$
	532.9	64		(E2) [a]	$19/2^- \rightarrow 15/2^-$
	670.9	47		(E2) [a]	$23/2^- \rightarrow 19/2^-$
	792.1	17		(E2) [a]	$27/2^- \rightarrow 23/2^-$

(continued)

Table 2 (continued)

La Isotope	E_γ	Relative Transition Intensity	$A_2 = G_2A_2(max)$	Multi-polarity	Transition Assignment
133	58.2	190		E1 [f]	$11/2^- \to 9/2^+$
	130.7	78		M1 [f]	$7/2^+ \to 5/2^+$
	346.4	7.4		M1	$9/2^+ \to 7/2^+$
	404.5	4.1		M2 [f]	$11/2^- \to 7/2^+$
	444.7	100		(E2) [a]	$15/2^- \to 11/2^-$
	477.0	170		E2 [f]	$9/2^+ \to 5/2^+$
	681.2	60		(E2) [a]	$19/2^- \to 15/2^-$
	789.1	21		(E2) [a]	$23/2^- \to 19/2^-$
135	119.4	20	$-.05\pm.04$	M1	$7/2^+ \to 5/2^+$
	133.4	48	$-.19\pm.02$	(M1) [b]	$25/2^- \to 23/2^-$
	202.0	86	$-.23\pm.02$	E1 [b]	$11/2^- \to 9/2^+$
	375.4	59	$.14\pm.02$	(E2) [b]	$19/2^- \to 15/2^-$
	379.3	54	$.15\pm.02$	(E2) [b]	$23/2^- \to 19/2^-$
	464.5	≤ 8			$(9/2^+ \to 7/2^+)$
	470.2	38	$-.47\pm.04$	(M2/E1 ≈ 1) [b]	$27/2^+ \to 25/2^-$
	583.9	100	$.21\pm.02$	E2 [b]	$9/2^+ \to 5/2^+$
	592.8	82	$.19\pm.02$	E2 [b]	$15/2^- \to 11/2^-$
137	168.8	100		E1	$11/2^- \to 9/2^+$
	781.6	87		E2	$15/2^- \to 11/2^-$
	824.6	95		E2	$9/2^+ \to 5/2^+$
	835.4	21		M1	$9/2^+ \to 7/2^+$
	1004	6.5		M2 + E3	$11/2^- \to 7/2^+$

[a] E2 cascade sequence assigned on systematics and comparison with doubly-even Ba isotope.

[b] Assigned from angular distribution data.

[c] Assigned from conversion-electron data of this work.

[d] Observed in β-decay from Ca.

[e] Assigned from conversion-electron work in ref. [11]).

[f] Assigned from conversion-electron work in ref. [19]).

Table 3

^{131}La conversion-electron data

E_γ		Theoretical						Expt.	Assignment
		M3	M2	M1	E3	E2	E1		
109	α_K	39	6.3	0.73	4.6	0.95		6.4*	M2
	K/(L + M)	1.8	3.9	6.1	0.40	1.9		5.0	M2
170	α_K		1.3	.21	1.0	.23	0.05	0.15*	M1
	K/(L + M)		5.4	6.2	1.0	3.0	6.3	5.1	M1

*Experimental α_K's evaluated assuming the 109 keV and 170 keV transitions have the same total intensities.

Table 4

^{133}La conversion data

E_γ		Theoretical M2	M1	E2	E1	Expt.[a]
404.5	α_K	.075	.021	.016	.0049	.07
477	α_K	.046	.014	.010	.0033	.012[a]

[a]Data from ref. 19).

Table 5

Isotope	Excitation Energy of $9/2^+$	core 2^+ energy + $5/2^+$ energy	$R = \frac{T(E2;9/2\to5/2)}{T(M1;9/2\to7/2)}$ $R_{exp}/R_{s.p.}$	$R = \frac{T(E2,7/2^+\to5/2^+)}{T(M1,7/2^+\to5/2^+)}$ $R_{exp}/R_{s.p.}$
139	–	1.595	–	3.5×10^3 †
137	836	828	1.7×10^3	–
135	584	605	4.7×10^3	3.9×10^3 †
133	477	464	3.4×10^3	4.9×10^3 †
131	414	382	0.8×10^3	–

†Data taken from ref. 24).

Figure Captions

Fig. 1. Schematic illustration of energy-level scheme for strongly-coupled $h_{11/2}$ particle in (oblate) $\Omega = 11/2$ state on left and (prolate) $\Omega = 1/2$ state on right (with decoupling parameter $a = -6$). For comparison, the level scheme of the doubly-even core is shown in the middle with the same moment-of-inertia.

Fig. 2. In-beam gamma-ray spectrum of $^{124}Te(^{11}B,4n)^{131}La$ taken with an 8 cm^3 planar Ge(Li) detector placed at 90° to the beam axis.

Fig. 3. In-beam and out-of-beam gamma-ray spectrum of $^{122}Te(^{11}B,4n)^{129}La$ taken with an 8 cm^3 planar Ge(Li) detector placed at 90° to the beam axis.

Fig. 4. Lower part of decay schemes for (a) ^{129}La, (b) ^{131}La, (c) ^{133}La. The references for the ^{133}La assignments are: a) this work, b) ref. [23]), c) ref. [24]), d) ref. [19]).

Fig. 5. Decay scheme for ^{135}La.

Fig. 6. Position of the band heads for the states in the odd-mass lanthanums.

Fig. 7. The bands based on the $11/2^-$ states in the odd-mass lanthanums compared to the ground-state bands in the corresponding doubly-even barium nuclei.

Fig. 8. The sequence of energy levels obtained by diagonalizing eq. (2) for various values of β. The lowest state of each spin up to $I = 23/2$ and the second $I = 11/2$ state is shown. The ordinate is the eigenvalue less the lowest $I = 11/2$ eigenvalue, in units of E_{2+} of the core, and the abscissa is β. The Fermi surface is taken below the set of orbitals for this calculation, corresponding to the case of the lanthanum nuclei.

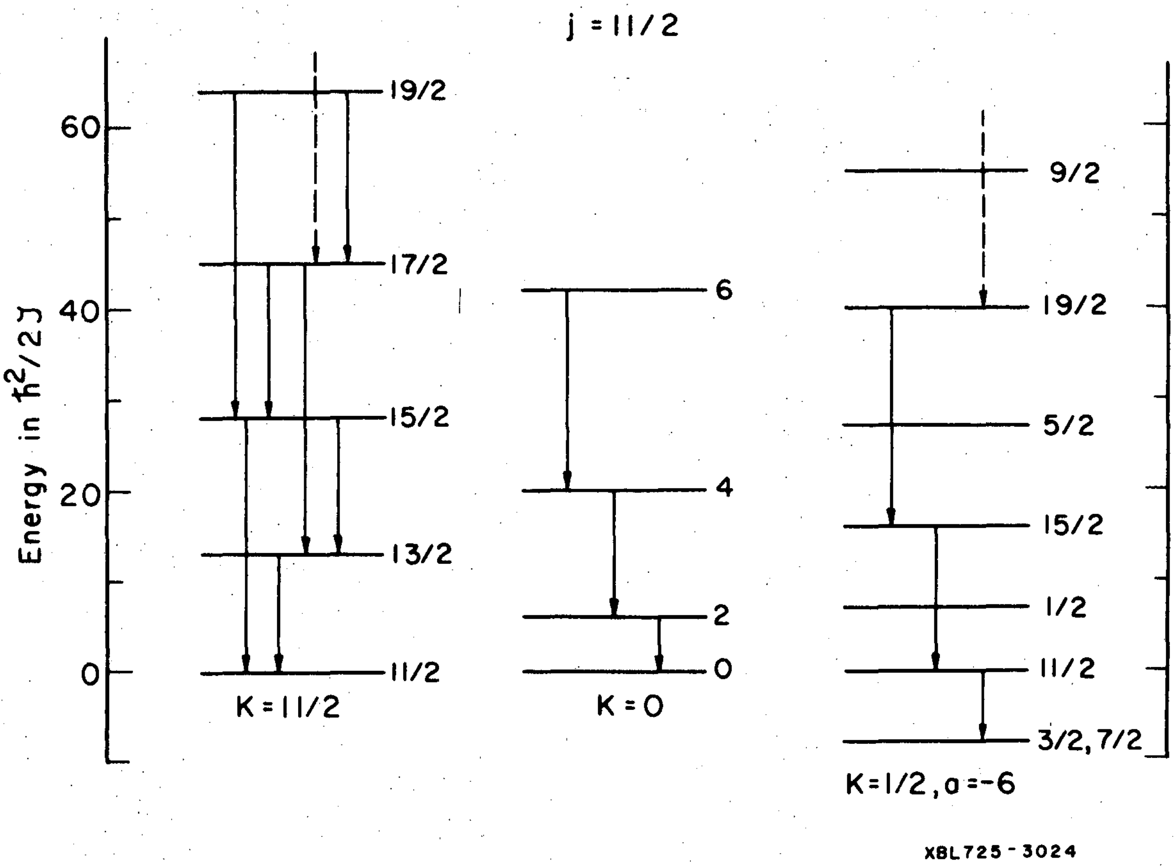
j = 11/2
Energy in ħ²/2J
60
40
20
0
19/2
17/2
15/2
13/2
11/2
K = 11/2
6
4
2
0
K = 0
9/2
19/2
5/2
15/2
1/2
11/2
3/2, 7/2
K = 1/2, a = -6
XBL725-3024

Fig. 1

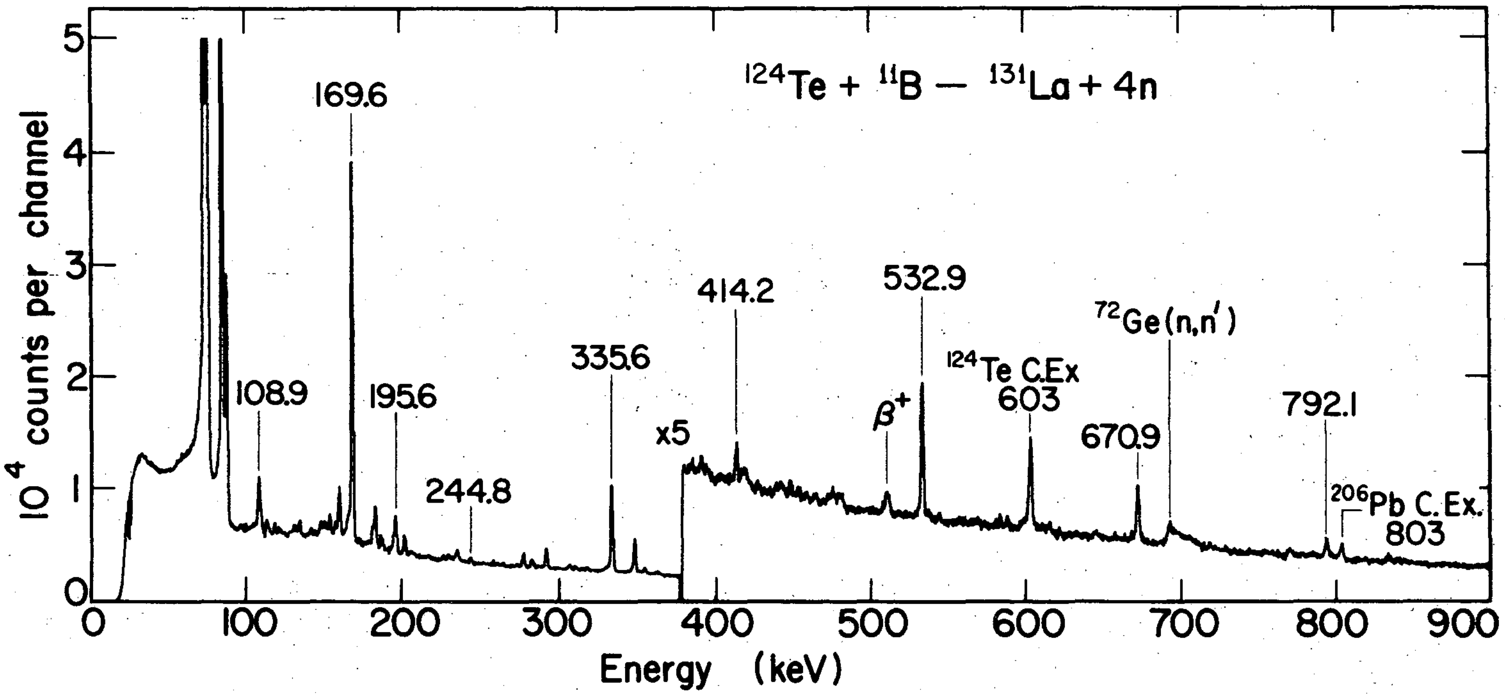

XBL735-3011

Fig. 2

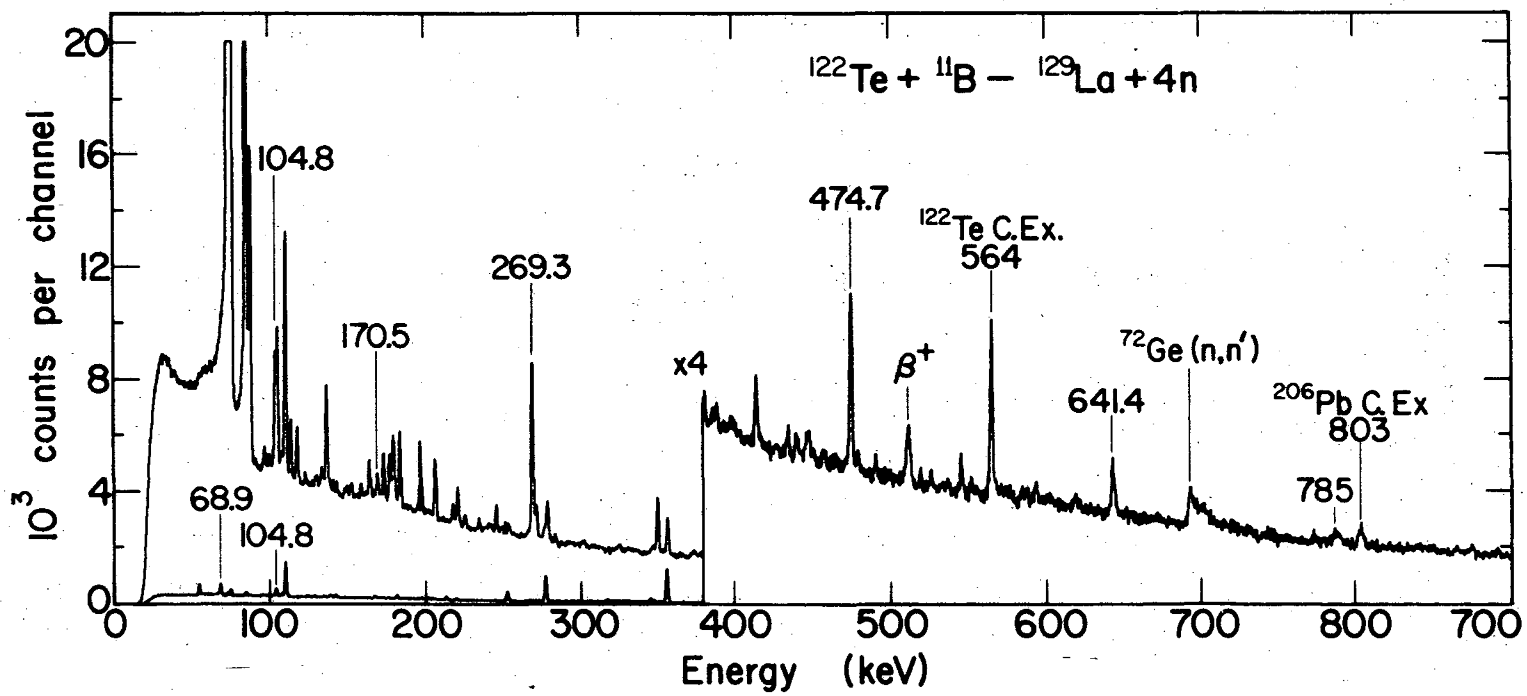

XBL735-3015

Fig. 3

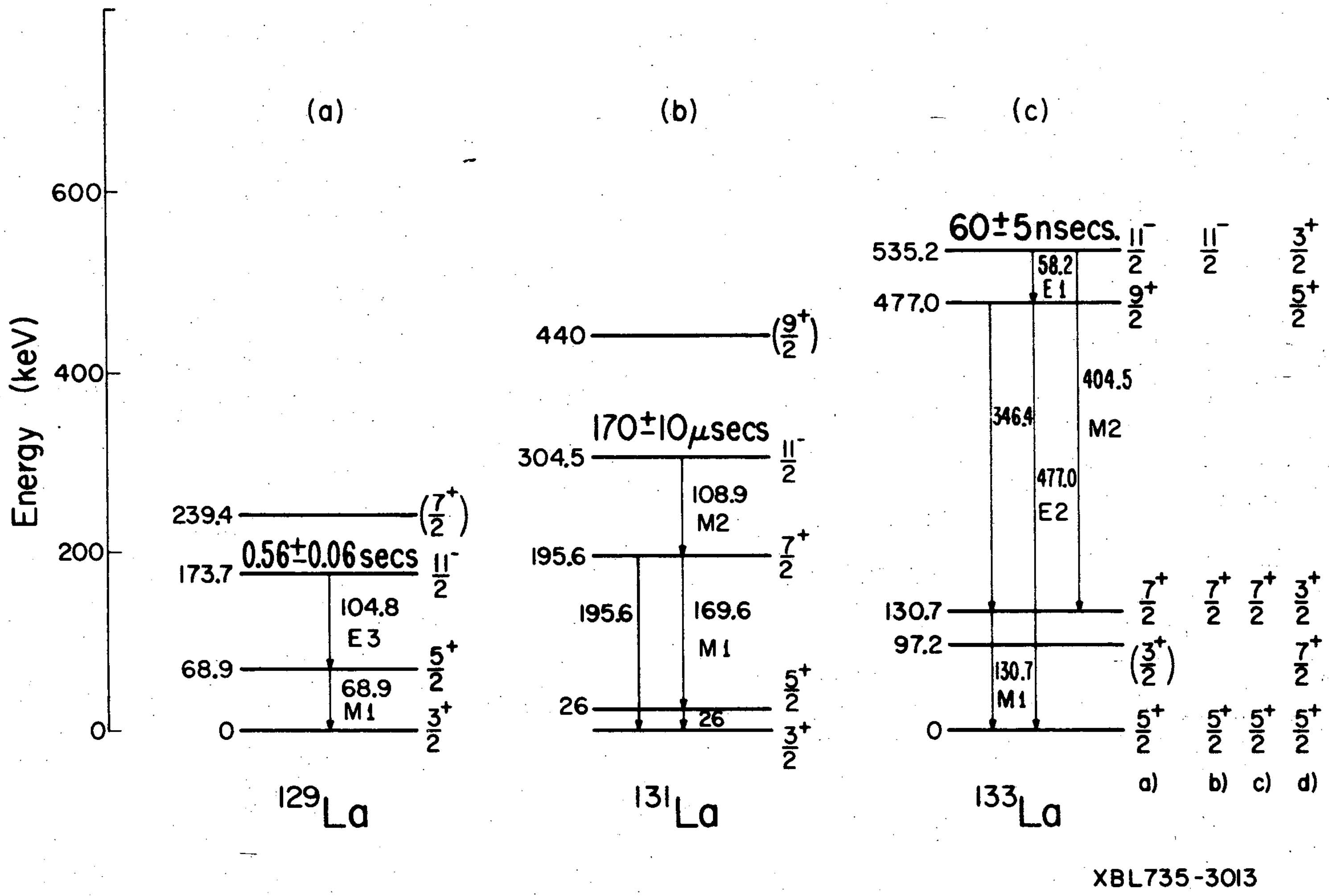

(a)
(b)
(c)
Energy (keV)
600
400
200
0
239.4
(7/2+)
0.56±0.06 secs
173.7
11/2−
104.8
E3
68.9
5/2+
68.9
M1
0
3/2+
129La
440
(9/2+)
170±10μsecs
304.5
11/2−
108.9
M2
195.6
7/2+
195.6
169.6
M1
26
5/2+
26
3/2+
131La
60±5nsecs.
535.2
11/2−
11/2−
3/2+
58.2
E1
477.0
9/2+
5/2+
404.5
M2
346.4
477.0
E2
130.7
7/2+
7/2+
7/2+
3/2+
97.2
(3/2+)
7/2+
130.7
M1
0
5/2+
5/2+
5/2+
5/2+
a)
b)
c)
d)
133La
XBL735-3013

Fig. 4

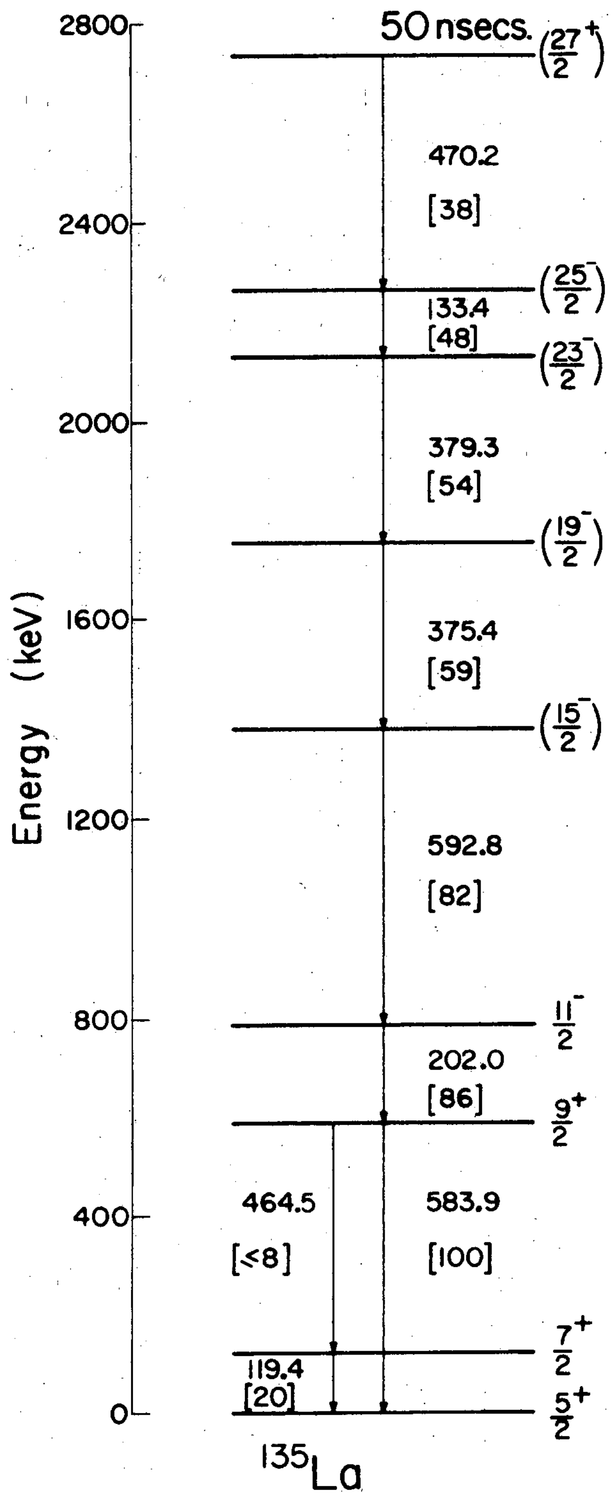

2800
2400
2000
1600
1200
800
400
0
Energy (keV)
50 nsecs.
(27+/2)
470.2
[38]
(25-/2)
133.4
[48]
(23-/2)
379.3
[54]
(19-/2)
375.4
[59]
(15-/2)
592.8
[82]
11-/2
202.0
[86]
9+/2
464.5
[≤8]
583.9
[100]
7+/2
119.4
[20]
5+/2
135La
XBL735-3012

Fig. 5

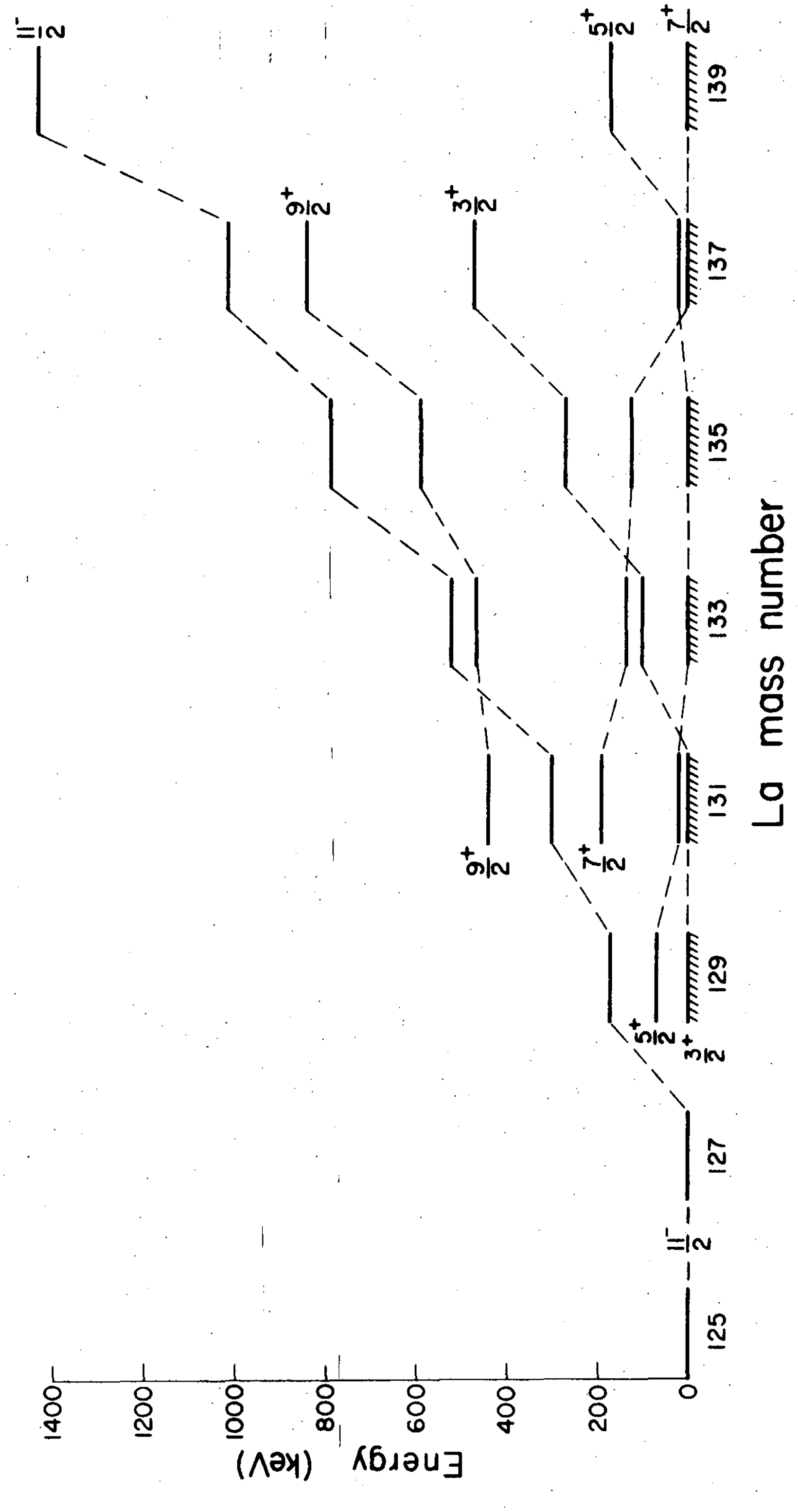

XBL735-3014

Fig. 6

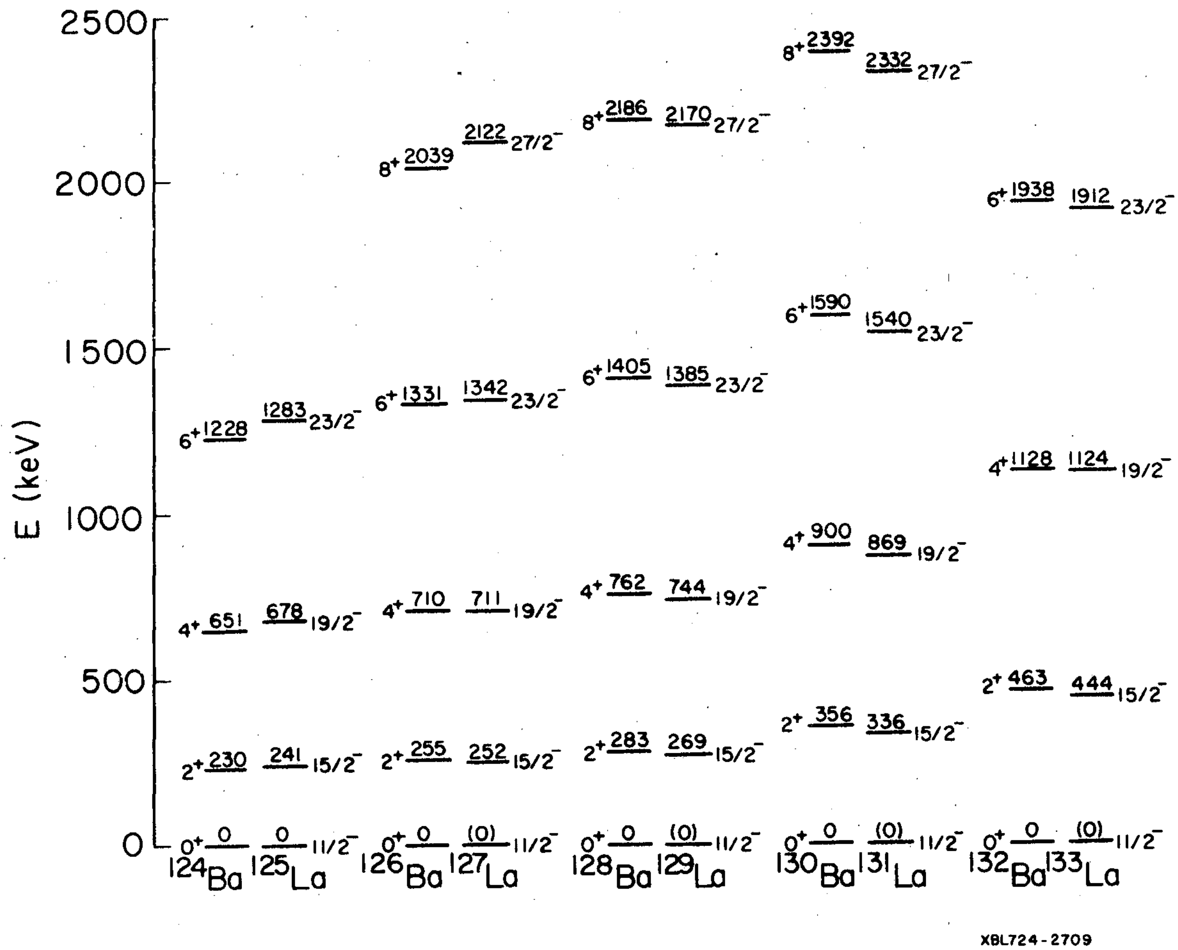
2500
2000
1500
1000
500
0
E (keV)
8+ 2039
2122 27/2−
8+ 2186
2170 27/2−
8+ 2392
2332 27/2−
6+ 1938
1912 23/2−
6+ 1590
1540 23/2−
6+ 1228
1283 23/2−
6+ 1331
1342 23/2−
6+ 1405
1385 23/2−
4+ 1128
1124 19/2−
4+ 900
869 19/2−
4+ 651
678 19/2−
4+ 710
711 19/2−
4+ 762
744 19/2−
2+ 463
444 15/2−
2+ 356
336 15/2−
2+ 230
241 15/2−
2+ 255
252 15/2−
2+ 283
269 15/2−
0+ 0
0 11/2−
0+ 0
(0) 11/2−
0+ 0
(0) 11/2−
0+ 0
(0) 11/2−
0+ 0
(0) 11/2−
124Ba 125La 126Ba 127La 128Ba 129La 130Ba 131La 132Ba 133La
XBL724-2709

Fig. 7

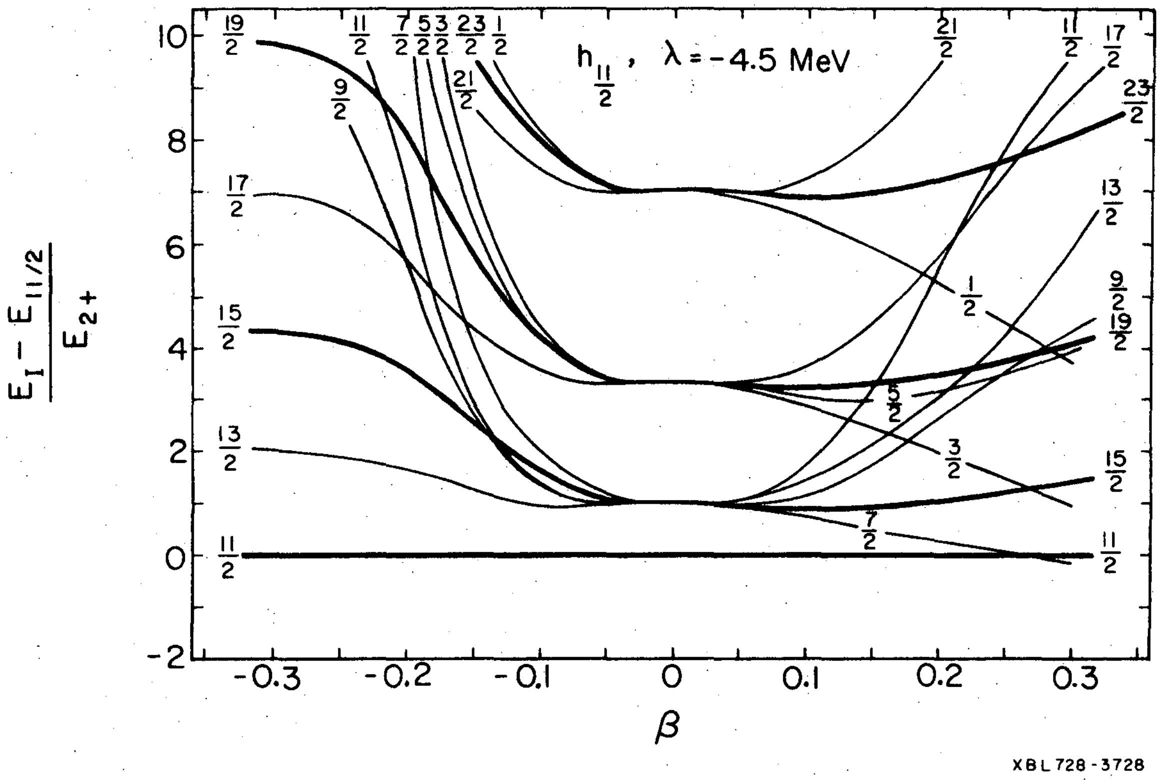

Fig. 8

TECHNICAL INFORMATION DIVISION
LAWRENCE BERKELEY LABORATORY
UNIVERSITY OF CALIFORNIA
BERKELEY, CALIFORNIA 94720